

Synthesis Of Double Lanthanide Doped Nano Ferrite Meta Material For Microstrip Patch Antenna Application

S.K.A.Ahamed Kandu Sahib¹, M.Suganthi², Vasant Naidu¹, S.Pandian³ and M.Sivabharathy^{*4}

¹Dept of ECE, Sethu Institute of Technology, Kariapatti- 626 115, India

²Dept of ECE, Thiagarajar College of Engineering, Madurai-620 015, India

³Defence Metallurgical Research Lab, Hyderabad-500 058, India

⁴Dept of Physics, Sethu Institute of Technology, Kariapatti- 626 115, India

*Corres.author: M.Sivabharathy

Abstract: A series of novel double lanthanide doped (Cerium, Ce³⁺ and Erbium, Er³⁺) nano magnesium meta ferrite material was synthesized by sol-gel route and sintered in a microwave furnace. For constructing Microstrip patch antenna of the as prepared material was studied to determine ϵ_r , $\tan\delta$, μ and χ , earlier it was seen that ϵ_r and $\tan\delta$ were high, due to the double doping ϵ_r , $\tan\delta$ and μ decreased significantly which was suitable for the designing the Micro Strip Patch Antenna at 3.1 GHz-10.6 GHz frequency range. The Structural and Size analysis of this as prepared material was investigated by X-ray Diffraction (XRD) and Scanning Electron Microscope (SEM) the size came to be 66-76 nm. In the further studies, both the dielectric constant and loss tangent were found to show a large in the value as compared to the earlier one. It was verified that the defined properties with extremely low permittivity and low loss factor with an improved DC resistivity were suitable for the material to be known as metamaterial. These Properties were further used to design and construct the Micro Strip Patch antenna with the improved directivity of 6.6 dB and the gain came to be -4.17 Db.

Keywords: SEM, VSM, low dielectric constant, Microstrip Patch antenna, Antenna

1. Introduction

In recent years, nano composite materials play the vital role to enhance the radiation performance of the antenna in 3.1 GHz to 10.6 GHz applications [1]. Ferrites being magnetic materials have a wide range of applications for high density magnetic data storage system, microwave absorbing material, gas sensor, magnetic resonance imaging contrast agents, targeted release of drugs etc. MgFe₂O₄ ferrites are partially inverse spinel with ferromagnetic property, since Mg²⁺ is anti ferrimagnetic with diffusible in nature. Therefore, its distribution in the crystal lattice site large depends on the synthesis conditions like precursor, pH condition, heat treatments [2, 3]. These preparation conditions directly affect the cation distribution which in turn reflects in the physical and chemical properties of ferrites to a greater extent. The structural, electric and magnetic properties of the ferrites are enhanced by substitution of different metal ions in its tetrahedral and octahedral sites [4, 5].

A variety of chemical synthesis methods are used for synthesizing nanosized spinel ferrites, such as, sol-gel, wet-chemical, co-precipitation, micro-emulsion, auto-combustion, hydrothermal and reverse micelle [2, 3, 6, 7]. The wet-chemical synthesis of high reactive powders has been proved to be an effective method for the synthesis of ferrites. However, it performs the calcinations at high temperature to obtain the final product of powder with expected crystal structure. Good stoichiometric control and production of ultrafine particles in

nano-range at relatively low temperature has attracted many researchers to choose sol-gel technique as preparation method [7].

The unusual magnetic, optical and electrical properties of rare-earth doped ferrites have been attracted the attention of many researchers in recent years. The rare-earth lanthanides are good electrical insulators with a high resistivity. The rare-earth is widely used to modify the structural, magnetic and electrical properties of the ferrites. A Strong correlation between the conduction mechanism and the dielectric behavior of the doped ferrites has been reported [8, 9]. The effects of the substituted rare earth ions like La, Sm, Gd, Dy, Yb, Er, Tb, Ce and Y in Fe^{3+} B site of ferrites have been investigated [10]. The substitution of large rare-earth ions in Fe^{3+} ions results in change in strain which induces structural distortion and there by modify the properties of samples [11]. This substitution results into high dc resistivity, very low electrical permittivity and low dielectric loss [12]. To further reduce the electrical permittivity and dielectric loss dual doping has been done. Therefore, in our present investigations, an attempt has been made to study the structural, magnetic property and behavior of localized electric charge carriers due to Ce^{3+} and Er^{3+} doping in magnesium ferrite to behave as metamaterials. This study offer valuable information which has not been reported. Moreover, by using this dielectric material for the substrate, a rectangular Microstrip patch antenna with the further reduction in size and increase in antenna directivity has been designed and the parameters related to the antenna performance are being discussed.

2. Experimental Procedure

Cerium and Erbium doped magnesium ferrite were prepared by sol-gel auto combustion method with different composition of x and y ($x=0.08, 0.06$ and 0.04 and $y = 0.04, 0.05$ and 0.04). Similar procedure discussed in our earlier studies [13] was used to prepare the $\text{MgCe}_x\text{Er}_y\text{Fe}_{2-x-y}\text{O}_4$ ferrites. X-ray powder diffraction (XRD) pattern was recorded for the as prepared ferrite samples by using the (PAN analytical, X' Pert Pro) diffraction spectrometer. The recorded X-ray pattern was used to conclude the respective diffraction planes of structure and helps to determine the crystalline size of these as-prepared ferrites. Scanning electron microscope (SEM; S3000-H, Hitachi, Japan) was used to obtain the SEM microscopic of as-prepared nano ferrite materials to determine the particle size. Energy dispersive analysis of X-ray (EDX) was done on Genesys 20 spectrophotometer (USA) which confirms the presence of element present in the as prepared doubly doped nano ferrites.

A vibrating sample magnetometer (VSM; 73009, Lakeshore, USA) was used to study the hysteresis loops of the as prepared ferrite materials. The four-probe method (DFM-RM, SES Instruments, and India) was used to study the temperature dependence of electrical resistivity in these ferrite samples. The dielectric resistance, relative permittivity and loss tangent of the as prepared ferrites was obtained employing N4L LCR meter (PSM 1735, England). These as prepared samples were converted in to polymers and sandwiched between the two plates of RT-DUROID. The dimensions of Microstrip patch antenna were calculated as shown below and finally the directivity and efficiency of the Microstrip patch antenna was obtained by using ADS simulation software.

Calculation of Microstrip Patch Antenna Dimensions:

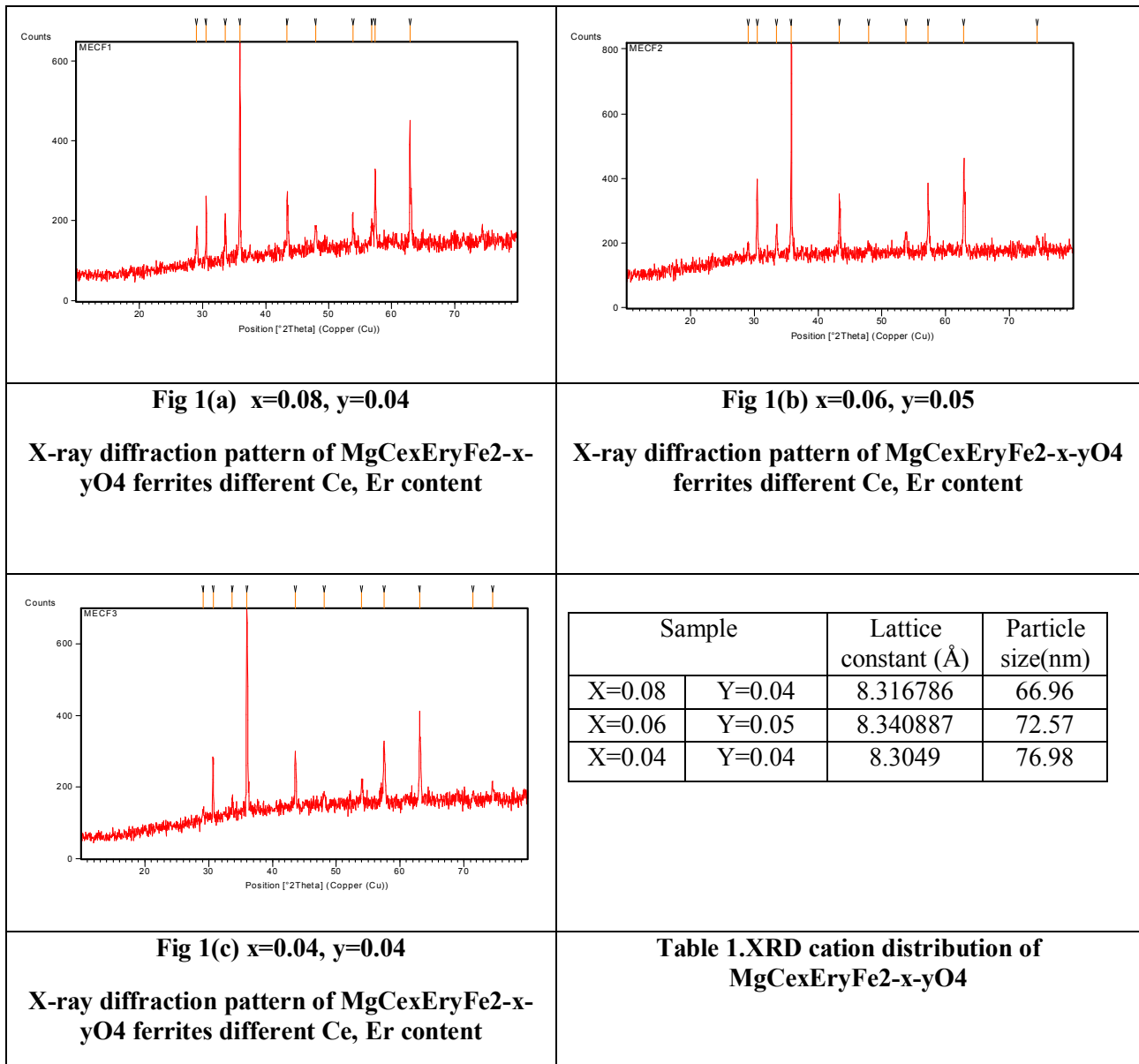
Using the relative dielectric constant ($\epsilon_r= 2.4540$) and thickness ($h=2.25\text{mm}$) of the dielectric material for the frequency ($f_0= 5.4$ GHz), the dimensions (L and W) of the rectangular Microstrip antenna had been calculated using EM-TALK Microstrip patch antenna calculator.

The Values was obtained,

Length (L) =16.43438m and Width (W) =21.1372m

3. Results and Discussion

The XRD pattern of the as-prepared $\text{MgCe}_x\text{Er}_y\text{Fe}_{2-x-y}\text{O}_4$ ferrites is shown in Fig. 1 (a, b, C).



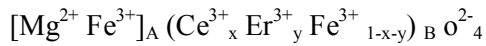
The observed XRD pattern confirms the formation of single phase spinel structure corresponding to the standard crystallographic phase as mentioned in JCPDS card No: 73-2211. Here the intensity peaks of the observed XRD pattern were coinciding with the peaks mentioned in JCPDS. Further the intensity of the XRD peak was found to be decreasing with the increase in doping concentration of Er^{3+} and Ce^{3+} this causes the difficulty in the process of crystallization with the increase in rare earth ions decrease in ionic radius [8, 10]. Here the shift in prominent peak (i.e., 311 peak) position due to the doping of Er^{3+} was seen. However, few extra reflections peaks were also present in the diffraction pattern due to oxides of doubly doped Cerium and Erbium ions [14].

The lattice parameter obtained from the XRD diffraction peaks were 8.3043, 8.3168 and 8.3409 \AA . It is seen that the lattice parameter increases linearly with the increase of Ce^{3+} and Er^{3+} ions. This confirms the increase in lattice parameter is due to the larger ionic radius of Ce^{3+} (1.15 \AA) and Er^{3+} (1.03 \AA) than those of host cation i.e., Mg^{2+} (0.86 \AA) and Fe^{3+} (0.69 \AA). The crystallite size of the as-prepared ferrites was also estimated from XRD pattern by using Scherer's formula ($D=0.94\lambda/\beta\cos\theta$)

Here λ was 1.5406 \AA . As it has been reported earlier that a crystallite size of ~ 50 nm is desirable for obtaining a suitable signal-to-noise ratio for switching applications [15]. Thus it confirms the application of this as prepared material will be useful for micro strip patch antenna construction. The increase in crystallite size with increase in concentration of Er^{3+} and Ce^{3+} is matched with the earlier reported results [16-18], it is mentioned that due to the larger bond energy of $Er^{3+}-O^{2-}$ and $Ce^{3+}-O^{2-}$ as compared to that of $Fe^{3+}-O^{2-}$ here more energy is needed to make Er^{3+} and Ce^{3+} ions to enter into the lattice for the formation of lanthanides

oxygen bonds. Thus it concludes that the lanthanide substituted ferrites have higher thermal stability relative to pure magnesium ferrites, but more energy is needed for the lanthanide substituted samples to complete crystallization and grow grain gradually.

Here the gradual increase in lattice parameter is attributed replacement of Mg²⁺ ions. However due to Er³⁺ and Ce³⁺ substitution the lattice constant is found to decrease than for the corresponding undoped samples. This supports the occupancy of Er³⁺ and Ce³⁺ on octahedral site. The similar results have been reported for rare earth element substitution for Ni-Zn ferrites [19].The Knowledge of the cation distribution and spin alignment is essential to understand the magnetic properties of spinel ferrite. The investigation of cation distribution helps to develop materials with desired meta properties which are useful for many device applications.



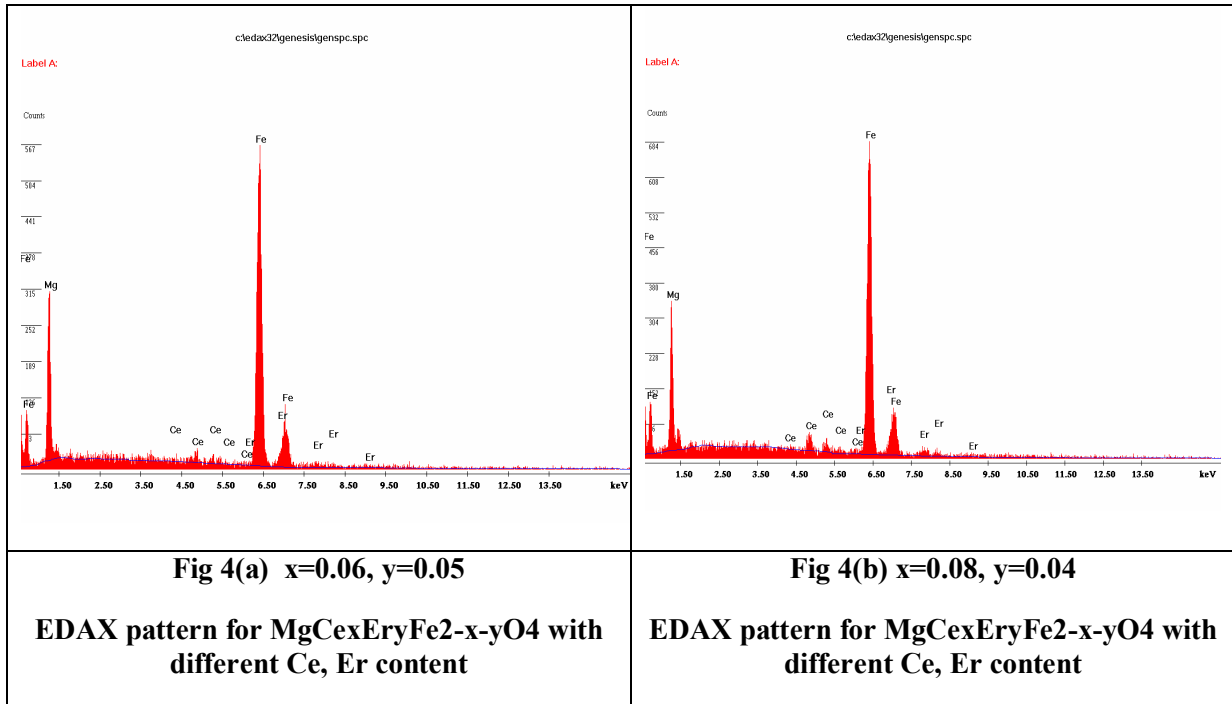
Where the brackets [] and () indicate the A site and B site respectively. Ce³⁺ Er³⁺ is an inverse spinel structure in which half of the ferric ions preferentially occupy the tetrahedral site (B sites) and the other half occupies the octahedral sites (A sites). On the other hand non-magnetic Mg ions prefer to occupy the tetrahedral sites.

The SEM micrograph confirms the nano phase of the crystallite shown in Fig. 2 (a, b, c). The analysis confirmed the microstructure of the sintered specimen. The Er³⁺ and Ce³⁺ doubly -doped specimens show a bi-phasic microstructure which is seen as the dark ferrite matrix grains along with the intense whitish grain at the grain boundary.

<p>Fig 2(a) x=0.08, y=0.04 SEM images of sintered MgCexEryFe2-x-yO4 with different Ce, Er content</p>	<p>Fig 2(b) x=0.06, y=0.05 SEM images of sintered MgCexEryFe2-x-yO4 with different Ce, Er content</p>																
	<table border="1"> <caption>Data for Fig 3: Susceptibility vs Permeability</caption> <thead> <tr> <th>Permeability</th> <th>Susceptibility</th> </tr> </thead> <tbody> <tr> <td>0</td> <td>1.001</td> </tr> <tr> <td>0.00002</td> <td>1.002</td> </tr> <tr> <td>0.00004</td> <td>1.003</td> </tr> <tr> <td>0.00006</td> <td>1.005</td> </tr> <tr> <td>0.00008</td> <td>1.006</td> </tr> <tr> <td>0.0001</td> <td>1.008</td> </tr> <tr> <td>0.00012</td> <td>1.009</td> </tr> </tbody> </table>	Permeability	Susceptibility	0	1.001	0.00002	1.002	0.00004	1.003	0.00006	1.005	0.00008	1.006	0.0001	1.008	0.00012	1.009
Permeability	Susceptibility																
0	1.001																
0.00002	1.002																
0.00004	1.003																
0.00006	1.005																
0.00008	1.006																
0.0001	1.008																
0.00012	1.009																
<p>Fig 2(c) x=0.04, y=0.04 SEM images of sintered MgCexEryFe2-x-yO4 with different Ce, Er content</p>	<p>Fig 3 Susceptibility vs Permeability</p>																

These activities are in accordance to the observation made for cerium doped magnesium ferrite [19] and the intense whitish grain boundary or the iron positions which are due to the occupation of the rare earth ions [20-21] can be seen in the Fig. 2 (a, b, c).

The EDAX spectra Fig. 4(a, b) obtained from the center of Er^{3+} and Ce^{3+} substituted Mg ferrite grains indicated the presence of Mg peaks at 4.50 to 5.50 keV and 6.50 to 7.50 keV, where as the Fe peaks are seen at 5.50 keV and 6.50 keV.



The vibrating sample magnetometer was used to obtain the magnetic measurements of the as prepared ferrites shown in Fig. 5. The obtained saturation magnetization (M_s) at room temperature was found to be 8.4611 emu/g and correspondingly the remnant magnetization (M_r) was 4.0061 emu/g. Magnetic Saturation was found to be 8.4611 emu/g and corresponding field of magnetization was 9500.0 G. The magnetic susceptibility (χ) was calculated by using the formula,

$$\chi = B/H$$

The value of χ came to be 0.000112279 and the corresponding value of μ was 1.00141 H/m. It has been that with the increase in doping content of Cerium Erbium the μ increases and χ decreases shown in Fig. 3.

As this magnetic $\text{Mg Ce}^{3+} \text{Er}^{3+}$ ferrite is subjected to a changing magnetic field, are time dependent effects happen to take place the magnetic moments reorient and the domain walls tends to move giving rise to two types of resonance. They are spin resonance and domain wall resonance. These spins will give rise to slow rotation which is directly related to frequency 10^7 - 10^8 s^{-1} . It is seen that this relaxation frequency is insufficient to attain the critical damping. For sintered MnCeEr ferrite the real part μ' , this is about 1000 in low frequency region. In these ferrite magneto composites, a magnetic inert component will get introduced thus causing not only the magnetic dilution but also a cut-off the magnetic circuit in the ferrite. Therefore, the permeability is reduced remarkably as the ferrite volume loading decreases. The other reason is due to the low volume loading composite sample have magnetic particles separated individually and the magnetic poles on each particle generate the demagnetizing field. The demagnetizing field reduces the induced magnetic moment more than that calculated from the volume loading. Therefore the permeability in low frequency region decreases with the concentration change from the sintered ferrite to the magneto composites. It is known that a step change of applied magnetic field will cause ferrites to respond with a simple relaxation of magnetization and the reciprocal of the complex susceptibility gives the simplest curve describe its spectrum. According to the globus model [22], the susceptibility spectrum is due to domain wall motion between points, such as grain boundaries. As the domain wall takes a two dimensional slice through the ferrites grain structure, the average diameter between grain boundaries is skewed towards the smaller grains. The high frequency portion of the susceptibility spectrum may be expected to show the effects of this distribution. In this region, the impedance of the material

is largely resistive, and will affect the ferrites intended for signal suppression to improve electromagnetic coefficient. The obtained values for M_s and M_r of lanthanide doped ferrites are greater than the earlier reported values for $MgFe_2O_4$ ferrites [9, 13, 21 and 23]. Since, the magnetic moment of Ce^{3+} and Er^{3+} ions is much greater than Fe^{3+} ions, a replacement of Fe^{3+} ions by Ce^{3+} or Er^{3+} ions at B site results in the increasing magnetic moment. The increase in saturation magnetization was observed with an increase in concentration of Er^{3+} and a decrease in concentration of Er^{3+} ions. The increase in magnetization of the prepared ferrites may explained by annihilation of a nonmagnetic layers (surface dead layers) due to the lanthanide doping. The coercivity of the prepared ferrites strongly depends on the particle size and anisotropy of the materials. In multi-domain particles, the magnetization reversal occurs due to the domain wall movement. As the domain walls move through a particle, they are pinned at grain boundaries. The additional energy is required for domain walls to continue the wall movement. Therefore, the doping of lanthanides creates more pinning sites and increases the coercivity of the ferrites. In the present investigation, the observed super-paramagnetic behavior in $MgCe_xEr_yFe_{2-x-y}O_4$ ferrite nanoparticles attributes to spin canting and surface spin disorder which occurred in these nano crystallized particles [20, 21]. These observed values for M_s and M_r of lanthanide doped ferrites suggest their suitability in applications like magnetic targeting and separators [21]

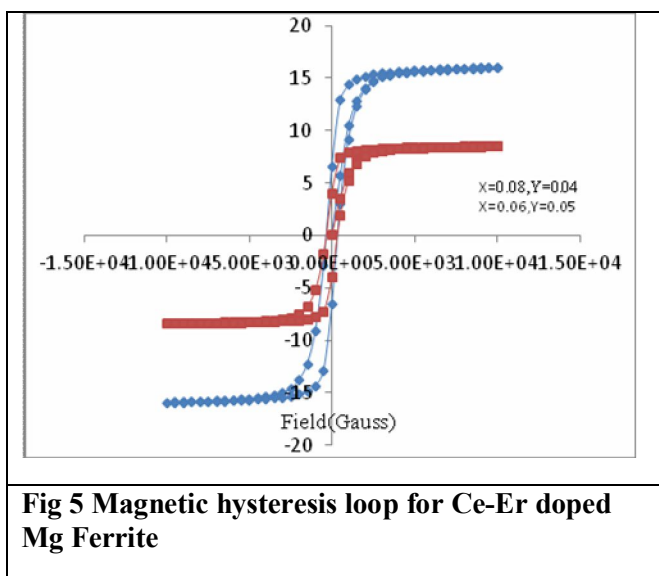
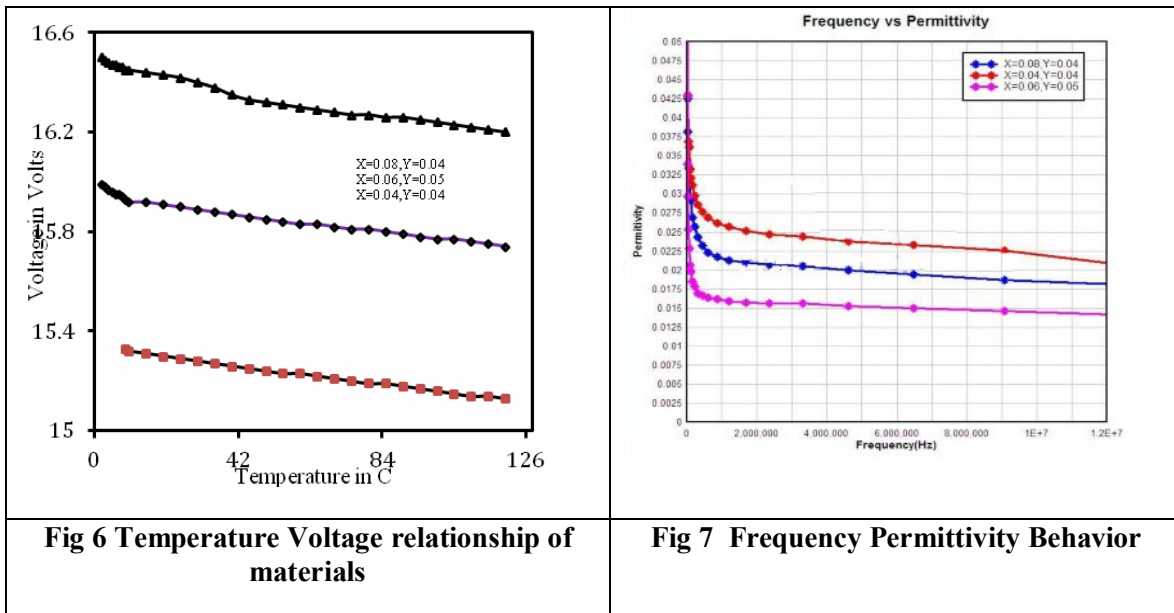


Fig 5 Magnetic hysteresis loop for Ce-Er doped Mg Ferrite

Small amount of Ce^{3+} and Er^{3+} doping has a great influence on magnetic properties. The hysteresis loops of Ce^{3+} and Er^{3+} substituted hexa-ferrite, calcined at $750\text{ }^\circ\text{C}$; show a behavior of the hard magnetic materials with high coercive force, as shown in Fig. 5. The variations of M_s and H_c values of $MgCe_xEr_yFe_{2-x-y}O_4$ are also shown in Fig. 5. As x increases, the value of M_s increases and reaches to the maximum, which coincides with some reports in the literature [24-26]. The increase in M_s could be contributed by the enhancement of hyperfine fields at 12k and 2b sites as strengthening in the $Fe^{3+} O Fe^{3+}$ super exchange interaction giving higher net magnetization [24]. As x increases, the effect of magnetic dilution is occurred with the changing of the Fe^{3+} (high spin) valence state to Fe^{2+} (low spin) state on +2 A site by substitution of the Mg^{2+} with Er^{3+} and Ce^{3+} ions.

The value of M_s at room temperature for the pure cobalt ferrite sample is 52.24 emu/g . The low value of saturation magnetization compared with that of the bulk can be understood on the basis of core-shell model, which explains that the finite size effects of the nano-particles lead to canting or non-co linearity of spins on their surface and thereby reducing the magnetization [27]. Semiconductor property of four probes was used to the study the temperature dependence of electric resistivity of the prepared $Mg Ce_x Er_y Fe_{2-x-y} O_4$ ferrites. It has been seen that there was no significant change in permittivity with the change with the change in temperature. Further it was seen that there was a drop in voltage with the increase in temperature (from 42 to 126 K) as shown in Fig. 6. The above observation conclude that the as prepared $Mg Ce_x Er_y Fe_{2-x-y} O_4$ ferrites behave as an n-type semiconducting material. Generally, it is reported that in polycrystalline ferrites the bulk resistivity rises from the combination of crystallite resistivity and the resistivity of crystallite boundaries [23,28and29]. Since, the boundary resistivity is much greater than that of the crystallite resistivity; the boundary has a greater influence on the dc resistivity. It has been seen that the decrease in dc resistivity with an increase in concentration of Ce^{3+} and a decrease in concentration of Er^{3+} in $Mg Ce_x Er_y Fe_{2-x-y} O_4$ ferrites is observed.



Here the partial reduction effects locally and give rise to the donor center [2-3, 8]. In these ferrite samples, the activation energy is also associated with the variation of mobility of charge carriers rather than concentration [20]. The charge carriers are considered to be localized on the ions or vacant sites giving rise to the conduction occurring from the hopping process. As this hopping depends upon the activation energy, which in turn is associated with the electrical energy barrier experienced by these mobile charge carriers [27-29].

The studies regarding the change in dielectric constant at room temperature for different composition of samples at various frequencies were made and are shown in Fig. 7. It was observed that the value of dielectric constant ranging from 0.015 to 0.025. From the figure it can be seen that the permittivity decreases with increase in frequency reaching constant value at higher frequencies. For low frequencies the dielectric constant is small, at intermediate frequencies its values begin to monotonically increase and eventually approach the values of the dielectric constant of this substrate. As the frequency of operation increases, most of the electric field lines concentrate in the substrate. At high frequency the change in permittivity of ferrite crystals is mainly due to atomic and electronic polarization in the ceramic grains. Here the presence of Fe²⁺ in ferrite materials always gives rise to high permittivity because Fe²⁺ has a larger polarization than Fe³⁺.

4. Application for Microstrip Patch Antenna

In the Microstrip patch antenna study, it was seen that with the decrease in ϵ_r the antenna directivity was found to be increasing. The as prepared dielectric material with permittivity 2.0511 was sandwiched between two glass epoxy materials, each with permittivity 5.42. The relative dielectric constant ϵ_r of the final product was found to be 2.4540 and the same material was used as the substrate for designing Microstrip patch antenna as in Fig. 8. The radiation parameters of the antenna were studied numerically using Advanced Design System simulation (ADS) software (Fig. 9).

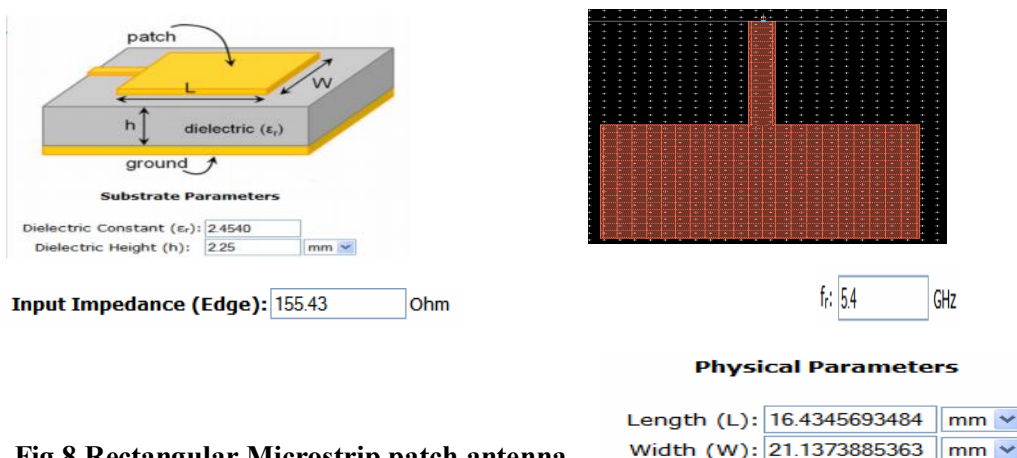


Fig 8 Rectangular Microstrip patch antenna

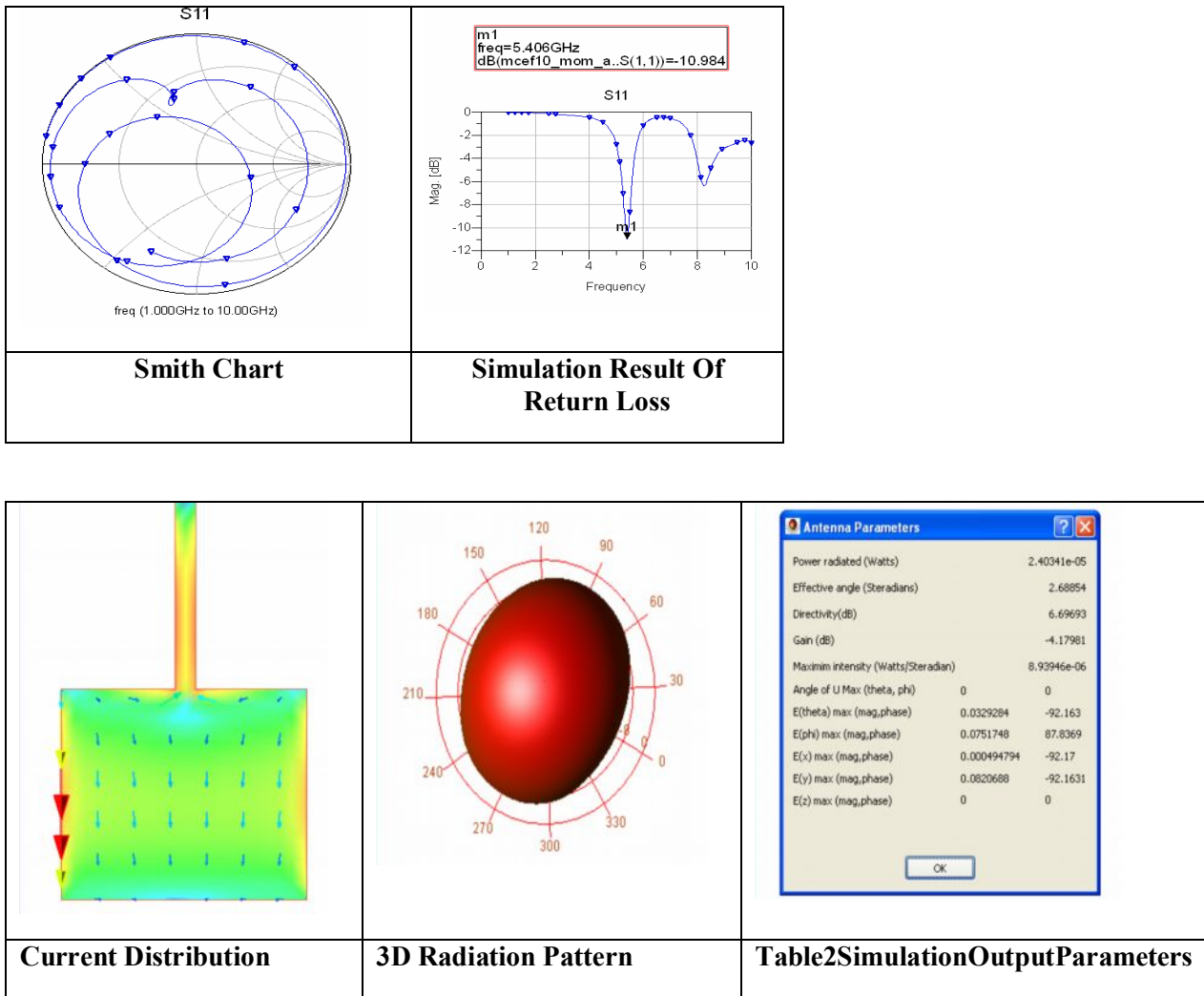


Fig 9 Antenna output

From the above results, it was found that the as prepared material would be suitable for constructing Microstrip patch antenna with high directivity. Also, for the designed antenna dimensions (L and W), the performance parameters like directivity and return loss of the constructed patch antenna was studied experimentally. These results were found to be better for high gain MSP Antenna.

5. Conclusion

In summary, Magnesium Cerium Erbium ferrite nano-crystalline were successfully prepared by sol-gel method. This nano crystalline $MgCe_xEr_yFe_{2-x-y}O_4$ meta ferrite powders were successfully synthesized with different doping levels. The Particle size, purity and crystalline size of respective powders was synthesized and confirmed by above XRD and SEM.

The ferrite powder was sintered at 1080°C; found sintering pellets was used for all measurements. The purity of the as-prepared ferrite samples was measured by the use of EDAX. The temperature dependent resistivity measurements were used to confirm the semiconducting behavior of the ferrite materials. By using LCR meter, the dielectric constant and loss tangent of ferrite materials was found. Further, we conclude that the above synthesized meta ferrite materials are suitable to be used as Microstrip patch antenna as it large increases the gain and directivity of antenna and this meta material can be further used for designing Photonic Band Gap antenna.

References

1. Shagar A.C. Wahidabanu R.S.D, New Design of CPW-Fed Rectangular Slot Antenna for Ultra Wideband Applications, International Journal of Electronics Engineering, Volume 2, 2010,pp. 69-73.
2. Pradeep A, Chandrasekaran G, FTIR study of Ni, Cu and Zn substituted nano-particles of MgFe_2O_4 , Materials Letters, Volume 60, 2006,pp. 371–374.
3. Pradeep A, Priyadharsini P and Chandrasekaran G, Sol–gel route of synthesis of nanoparticles of MgFe_2O_4 XRD, FTIR and VSM study, Journal of Magnetism and Magnetic Materials, Volume 320,2008, pp. 2774–2779.
4. Kulkarni R.G, Joshi H.H, Magnetic properties of $\text{MgZnFe}_2\text{O}_4$ System by Mossbauer Spectroscopy, Solid State Communication, Volume 53, 1985,pp. 1005-1008.
5. Gadkari A.B, Shinde T.J, Vasambekar P.N, Structural and magnetic properties of nanocrystalline Mg Cd ferrites prepared by oxalate co-precipitation method, Journal of Materials Science: Materials in Electronics, Volume 21, 2010,pp. 96-103.
6. Yue Z, Li L, Zhou J, Zhang H, Gu Z, Preparation and characterization of Ni Cu Zn ferrite nanocrystalline powders by auto-combustion of nitrate–citrate gels Materials Science and Engineering: B, Volume 64, 1999,pp. 68–72.
7. Candace T. Seip, Everett E. Carpenter, and Charles J. O'Connor, Magnetic Properties of a Series of Ferrite Nano-particles Synthesized in Reverse Micelles, IEEE Transactions on Magnetics, 1998,Volume 34.
8. Samy A.M, Gomaa E. and Mostafa N, Study the Properties of Cu-Zn Ferrite Substituted with Rare Earth Ions by Using Positron Annihilation Analysis, The Open Ceramic Science Journal, Volume 1, 2010,pp. 1-4.
9. ZHOU Chunhui, ZHU Yifeng, LIU Huazhang, Effect of Samarium on methanation resistance of activated carbon supported ruthenium catalyst for ammonia synthesis, Journal of Rare Earths, Volume 28,2010, pp. 552-555.
10. Sattar A.A. and. El-Shokrofy K.M, Rare Earth Doping Effect on the Electrical Properties of Cu-Zn Ferrites, Phys. IV France, Volume 07, 1997,pp. C1-245-C1-246.
11. Said M. Z, Hemeda D. M, Abdel kader S and Farag G. Z, Structural, Electrical and Infrared Studies of Ni 0.7 Cd 0.3 Sm Fe_2O_4 Ferrite, Turk J Phys Volume 37, 2007,pp. 41-50.
12. Jagdish Chand, Singh M., Electric and dielectric properties of Mg Gd 0.1 Fe 1.9 O_4 ferrite, Journal of Alloys and Compounds, Volume 486, 2009,pp. 376–379.
13. Vasant Naidu, et,al, Synthesis and characterization of novel nano ceramic magnesium ferrite doped with Samarium and Dysprosium for designing-micro strip patch antenna, Defect and Diffusion Forum, Volume 332, 2012,pp. 35 –50.
14. Cui-Ping Liu, Ming-Wei Li, Zhong Cui, Juan-Ru Huang, Yi-Ling Tian, Tong Lin, Wen-Bo Mi, Comparative study of magnesium ferrite nanocrystallites prepared by sol–gel and co precipitation methods, Journal of Materials Science, Volume 42, 2007,pp. 6133-6138.
15. Harish V.J, et,al, Recent Advances in Processing and Applications of Microwave ferrites, Journal of Magn and Magn Mater, Volume 321,2009, pp. 2035-2047.
16. Tok A.I.Y., et, al, Hydrothermal synthesis and characterization of rare earth doped ceria nanoparticles, Material Science and Engineering A, Volume 466, 2007,pp. 223-229.
17. Wu N.C., et,al, Effect of pH of medium on hydrothermal synthesis of nano crystalline cerium (IV) oxide powders, Journal of American Ceramics Soc, Volume 85, 2002,pp. 2462-2468.
18. Hirano M., Kato E., Hydro Thermal synthesis of Nano Crystalline Cerium(IV)Oxide Powders, Journal of American Ceramics Soc, Volume 82, 1999,pp. 786-788.
19. Rezlescu N, Rezlescu E, Pasnicu C, and Craus M.L, Effect of the rare-earth ions on some properties of nickel-zinc ferrite, J. Phys. Condens. Matter, Volume 6,1994,pp. 5707.
20. Jagdish Chand, et,al, Effect of Gd^{3+} doping on magnetic, electric and dielectric properties of Mg Gd $x\text{Fe}_2-x\text{O}_4$ ferrites processed by solid state reaction technique Journal of Alloys and Compounds Volume 486, 2009,pp. 376–379.
21. Ashok Gadkari, TukaramShinde, PramodVasambekar, Influence of rare-earth ions on structural and magnetic properties of CdFe_2O_4 ferrites, Rare Metals, Volume 29, 2010, pp. 168-173.
22. Globus A., Duplex P., Initial Susceptibility of Ferro Magnetic Materials and Topography of Domain Walls, Physica Status Solidi(b),Volume 31, 1969,pp.765-774.
23. Dascalu G., et,al, Structural, electric and magnetic properties of Co Fe 1.8 RE 0.2 O_4 (RE=Dy, Gd, La) bulk materials, Journal of Magnetism and Magnetic Materials, Volume 333,2013, pp. 69–74.

24. Ounnunkad S., Improving magnetic properties of barium hexa ferrites by La or Pr substitution, Solid State Communications, Volume 138,2006, pp. 472–475.
25. Liu Y., et,al, Preparation and magnetic properties of La-Mn and La-Co doped barium hexaferrites prepared via an improved co-precipitation/molten salt method, Journal of Magnetism and Magnetic Materials, Volume 322, 2010,pp. 3342–3345.
26. Ounnunkad S., Winotai P., Phanichphant S., Effect of La doping on structural, magnetic and micro structural properties of $Ba_{1-x}La_xFe_{12}O_{19}$ ceramics prepared by citrate combustion process, Journal of Electro ceramics, Volume 16, 2006,pp. 357–361.
27. Manoj Kumar and Yadav K L, Study of dielectric, magnetic, ferroelectric and magneto electric properties in the $PbMn_xTi_{1-x}O_3$ system at room temperature, J. Phys.: Condens. Matter,2007,19 242202.
28. Wang D. H., Goh W. C., Ning M., and Ong C. K.,Effect of Ba doping on Magnetic, ferroelectric, and magneto electric properties in mutiferic $BiFeO_3$ at room temperature, Appl. Phys, Volume 88,2006,212907.
29. Yamada S. and Otsuki E., Analysis of eddy current loss in Mn–Zn ferrites for power supplies, J. Appl. Phys, Volume 81, 1997,4791.
30. N. M. Deraz, A. Alarifi, Microstructure and Magnetic Studies of Zinc Ferrite Nano-Particles, Int. J. Electrochemical. Sci., 2012,pp. 6501 – 6511.
